

# EMOE: A Framework for Out-of-distribution Uncertainty Based Rejection via Model-Agnostic Expansive Matching of Experts

**Yunni Qu**<sup>1</sup>, **James Wellnitz**<sup>2</sup>, **Dzung Dinh**<sup>1</sup>, **Bhargav Vaduri**<sup>1</sup>, **Alexander Tropsha**<sup>2</sup>, **Junier Oliva**<sup>1</sup>

Department of Computer Science, University of North Carolina at Chapel Hill

201 S Columbia St, Chapel Hill, NC 27599 <sup>1</sup>

Eshelman School of Pharmacy, University of North Carolina at Chapel Hill

301 Pharmacy Lane, Chapel Hill, NC 27599 <sup>2</sup>

## Abstract

Expansive Matching of Experts (EMOE) is a novel framework that utilizes support-expanding, extrapolatory pseudo-labeling to improve prediction and uncertainty based rejection on out-of-distribution(OOD) points. EMOE utilizes a diverse set of multiple base experts as pseudo-labelers on the augmented data to improve OOD performance through multiple MLP heads (one per expert) with shared embedding train with a novel per-head matching loss. Unlike prior methods that rely on modality-specific augmentations or assume access to OOD data, EMOE introduces extrapolatory pseudo-labeling on latent-space augmentations, enabling robust OOD generalization with any real-valued vector data. In contrast to prior modality agnostic methods with neural backbones, EMOE is model-agnostic, working effectively with methods from simple tree-based models to complex OOD generalization models. We demonstrate that EMOE achieves superior performance compared to state-of-the-art method on diverse datasets in single-source domain generalization setting.

## 1 Introduction

It is well-known that the generalization capabilities of models can be severely limited when tested on out-of-distribution (OOD) data that deviates from the training-time distribution (Torralba and Efros 2011; Liu et al. 2021; Freiesleben and Grote 2023). This, in turn, affects many real-world applications where models may be evaluated on distribution-shifted data during deployment. For instance, these issues commonly arise in medical applications where patient distributions at inference time may deviate from the training data (Lee, Yin, and Zhang 2023). A potential strategy for the safe deployment of models in real-world applications is to employ novelty-based rejection (Dubuisson and Masson 1993; Hendrickx et al. 2024), where predictions are rejected whenever the model is evaluated on an instance that deviates from the data distribution seen during training. While such approach is appropriate in certain scenarios (e.g., when a human can easily intervene upon rejection), this prevalent strategy is overly conservative as it foregoes any potential extrapolation<sup>1</sup> by design. That is, novelty-rejection

forbids any form of extrapolation (predictions outside of the training data support), even when the model may be capable.

**Motivation & Broader Impacts** As a motivating example, consider a virtual screening application in drug discovery that aims to identify potential targets in molecules with machine learning, where a model must predict the properties of novel molecules that are often substantially different from previously characterized compounds. This requires models to generalize beyond the support of the training data, an ability referred to as "scaffold hopping" (Hu, Stumpfe, and Bajorath 2017) to identify structurally distinct candidates with desirable properties. However, most existing novelty-based rejection methods are designed to forbid extrapolation, restricting predictions to regions well-supported by the training data (Dubuisson and Masson 1993). This conservative approach, while ensuring reliability within known domains, fundamentally limits the discovery of novel candidates, which is the primary objective in drug discovery. Moreover, because experimental validation of candidate molecules is expensive and resource-intensive (Serrano et al. 2024), it is crucial to predict effectively on OOD instances while providing accurate predicted confidences. To manage cost only a small fraction of candidates should be selected for further laboratory tests. The use of models with poor confidence filtration will result in false positives that waste resources on unsuccessful experiments where screened molecules do not present desirable properties. Therefore, the success of discovery relies on the quality of high-confidence predictions on OOD data. We focus on the single source generalization setting (Qiao, Zhao, and Peng 2020) because it realistically reflects the constraints in practical virtual screening workflows where only a single labeled data set, often centered on a narrow chemical space, is available for training. Therefore, developing models that generalize from a single source to OOD drug candidates, while providing reliable confidence estimates, is a necessary direction for robust and cost-effective drug discovery.

**Aim** This work aims to improve the extrapolative capabilities of predictive models in single source domain generalization setting, with a focus on performance metrics such as AUROC and AUPRC. Moreover, we emphasize a model's ability to produce trustworthy confidences on OOD points and reject unreliable predictions based on predicted confidences. To do so, we develop a *general*, modality- and

<sup>1</sup>We use the term extrapolation to loosely encompass prediction outside of the training data distribution support (without consideration of the data's convex-hull).

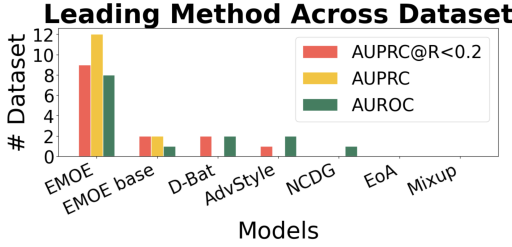


Figure 1: Tally of datasets where respective methods lead in metrics: AUPRC for recall  $< .2$  (AUPRC@R  $< .2$ ), AUPRC, & AUROC. (See further details in §4 and Appx.B.)

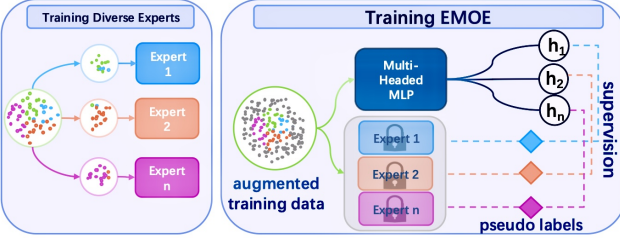


Figure 2: EMOE takes a 2-stage training approach. Stage 1 trains diverse base experts based on different subset of the training data (left). Stage 2 trains Multi-Headed Neural Network with pseudo labels on augmented data provided by the base experts (right).

model-agnostic end-to-end framework, ensuring maximum applicability to real-valued vector data and variety of models. To evaluate the model confidence, we propose a novel metric: area under precision/recall curve at recall less than  $\tau$  (AUPRC@R  $< \tau$ ). This metric specifically measures a model’s ability to accurately predict positive examples in its most confident predictions (e.g., see motivation for discussion on relevance to cheminformatic virtual screening). In contrast with prior work that depends heavily on modality-specific augmentations (e.g. for images (Yun et al. 2019), etc.) and/or the availability of multiple domains (Ding et al. 2022; Jang et al. 2023; Dou et al. 2019), our approach is fundamentally independent of data modality. Unlike prior modality-agnostic methods such as MODALS (Cheung and Yeung 2021) that is modular or MAD (Qu et al. 2023) that is effective with complex neural architectures, EMOE is compatible with a broad spectrum of models and provides an end-to-end framework that not only generates extrapolated data, but also effectively integrates them into training through diverse pseudo labeling via a novel per-head matching-based learning objective.

**Contributions** In this work, we propose a new method for single source domain generalization – EMOE, designed to extrapolate effectively and yield reliable uncertainty estimates in high-confidence regions through a novel training scheme using a multi-headed network based on matching augmented (expanded) data (see Fig. 2).

Our key contributions are: (1) We develop a straightforward but effective strategy that yields a strong, diverse set of base experts for self-training. (2) We propose a

novel training loss for multi-headed neural network architectures—composed of a per-head matching loss and a mean-matching regularization loss—to ensure both diversity (via per-expert supervision) and consistency (via ensemble agreement). (3) We introduce AUPRC@R  $< \tau$ , the normalized area under the precision-recall curve below a conservative threshold  $\tau$ . While  $R$  denotes recall in the metric name, we define the formal expression using a recall variable  $r$ :

$$\text{AUPRC@R} < \tau = \frac{1}{\tau} \int_0^\tau \text{Precision}(r) dr \quad (1)$$

This novel metric measures a model’s ability to predict confidence of true positive examples in its most confident predictions. (4) We show state-of-the-art (SOTA) performance in rejecting predictions based on estimated confidences, evaluated using AU{PR,RO}C-based metrics (see Fig. 1) in a single-source generalization setting (Qiao, Zhao, and Peng 2020). (5) We conduct several ablations to better understand the keys to EMOE’s success; moreover, by ablating the type of base experts, we show EMOE’s broad ability to improve over a model-agnostic set of experts.

## 2 Related Work

**Domain Generalization** Domain generalization (DG) aims to learn a model that is able to generalize to multiple domains. A typical approach is to learn a domain invariant representation across multiple source domains. Domain invariant representation learning can be done by minimizing variations in feature distributions (Li et al. 2018; Ding et al. 2022) and imposing a regularizer to balance between predictive power and invariance (Arjovsky et al. 2019; Koyama and Yamaguchi 2020). Another line of research incorporates data augmentation to improve generalizability. Basic transformations like rotation and translation, varying in magnitude, are commonly used on images to diversify the training data (Cubuk et al. 2019; Berthelot et al. 2020). More sophisticated augmentation techniques have recently surfaced: (Zhang et al. 2018) introduced mixup, which linearly combines two training samples; (Yun et al. 2019) proposed Cut-Mix, blending two images by replacing a cutout patch with a patch from another image; (Zhong et al. 2022) adversarially augment images to prevent overfitting to source domains. We focus on augmentations that are general and applicable across modalities. (Tian et al. 2022) introduced NCDG, which uses simple augmentations along with a loss function that maximizes neuron activity during training while minimizing standard classification loss. Their method minimizes the difference in the gradient of a coverage loss between standard training instances and augmented training instances.

**Self-Training** Self-training uses an earlier model to pseudo-label unlabeled data, which is then added to the training set for subsequent model updates. The concept of pseudo-labeling was initially proposed by (Lee 2013), suggesting a direct approach to retaining instances where the model has high prediction probabilities. Following (Lee 2013), (Zou et al. 2018) proposed selecting a proportion of the most confident unlabeled points instead of using a fixed

threshold. Later works combined pseudo-labeling with curriculum learning, dynamically adjusting class-wise thresholds over time to incorporate more informative samples (Cascante-Bonilla et al. 2020; Zhang et al. 2021). Another line of work improves pseudo-labeling robustness by promoting diversity in the labelers. (Ghosh et al. 2021) used model ensembles as teachers, while (Xie et al. 2019) added noise via Dropout (Srivastava et al. 2014) and data augmentation. FixMatch (Sohn et al. 2020) generates pseudo-labels from weakly augmented samples to supervise training on the corresponding strongly augmented samples. EMOE novelly leverages pseudo-labels by assigning each student head to a different expert, encouraging diversity, while aligns the ensemble prediction for consistency via a novel loss.

**Selective Classification** Reject option methods (or selective classification) aim to identify inputs where the model should abstain from predicting. Many approaches apply post hoc processing: after training, a rejection metric—such as the model’s predicted probability—is computed, and predictions below a set threshold are rejected (Stefano, Sansone, and Vento 2000; Fumera, Roli, and Giacinto 2000). Building upon these works, (Devries and Taylor 2018) proposed to train a confidence branch alongside the prediction branch by incentivizing a neural network to produce a confidence measure during training; (Geifman and El-Yaniv 2017) proposed a method for constructing a probability-calibrated selective classifier with guaranteed control over the true risk. Recently, methods adopting end-to-end training approaches have been proposed (Thulasidasan et al. 2019; Ziyin et al. 2019; Geifman and El-Yaniv 2019). In these works, an extra class is added when predictions are made. If the extra class has the highest class probability for a sample, the sample is rejected. Most reject-option approaches are geared towards in-distribution rejection and utilize novelty-rejection when encountering any OOD points (Torralba and Efros 2011; Liu et al. 2021; Freiesleben and Grote 2023); instead, we propose to learn better conditional output probabilities on OOD data for more effective, capability-aware rejection.

**Ensemble Modeling** Ensembles utilize a diverse set of models jointly for better performance. Early methodologies for ensembles aggregate (bag) predictions from all models (Dietterich 2007; Kussul et al. 2010) or a subset of the models in the ensemble (Jordan and Jacobs 1993; Eigen, Ranzato, and Sutskever 2013). In the OOD setting, prior works addressed this problem by enforcing prediction diversity on OOD data (Pagliardini et al. 2023), ensembling moving average models (Arpit et al. 2022a), training an ensemble of domain specific classifiers (Yao et al. 2023), and training diverse model heads within a single network by maximizing disagreement on unlabeled OOD data (Lee, Yao, and Finn 2022). EMOE adopts a multi-headed architecture that produces an ensemble to improve predictions on OOD data.

### 3 Method

Our approach, EMOE, consists of three core components: (1) training a diverse set of base experts; (2) generating extrapolatory samples via latent space augmentation; and (3) training a multi-headed network to match expert predictions on both ID and expanded data. This section de-

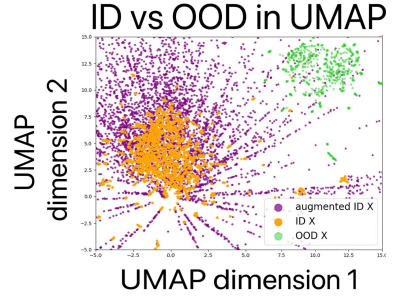


Figure 3: Expansion in UMAP space: ID points (orange) are augmented (purple) and expand the distributional support towards the OOD (green).

scribes each step in detail. Throughout, we assume the ‘single-source’ generalization setting (Qiao, Zhao, and Peng 2020), where we observe a single in-distribution (ID) training dataset  $\mathcal{D} = \{(x_i, y_i)\}_{i=1}^N$ , and instances are drawn *iid*  $(x_i, y_i) \sim \mathcal{P}_{\text{in}}$  without any accompanying environmental-/domain/source information *nor any labeled/unlabeled OOD instances*. For simplicity, we write to the binary classification case,  $y_i \in \{0, 1\}$ , but our methodology is easily extendable to other supervised tasks. We design our method to work in general, non-modality specific<sup>2</sup> (e.g., image, text, audio) settings, i.e.,  $x_i \in \mathbb{R}^d$ .

#### 3.1 Base Collection of Experts

EMOE leverages a set of diverse initial experts  $\{g_k\}_{k=1}^K$ , s.t.  $g_k : \mathbb{R}^d \rightarrow \{0, 1\}$ , to guide the training of a secondary model by providing pseudo-labels. There are many mixture of experts (Jordan and Jacobs 1993; Eigen, Ranzato, and Sutskever 2013) and ensembling (Arpit et al. 2022a; Dietterich 2007; Pagliardini et al. 2023; Yao et al. 2023) methods available, EMOE utilizes a collection of strong base-learners by sub-selecting on both instance and feature subspace, encouraging diversity by specializing experts on distinct regions and views of the latent representation space.

#### 3.2 Expansive Augmentation of Training Data

To train models capable of extrapolating to OOD samples, we need to expose them to data that lie outside the support of the training distribution. To reason about the support of the training data, and how to *expand* past it, we propose to leverage a latent factor space,  $\varphi : \mathbb{R}^d \mapsto \mathbb{R}^s$ . While learning semantically meaningful latent factor spaces remains an active area of research, we observed strong performance utilizing autoencoding techniques (see § 4), which carry a corresponding decoder  $\gamma : \mathbb{R}^s \mapsto \mathbb{R}^d$ . Without loss of generality, we consider centered latent spaces such that  $\mathbb{E}[\varphi(X)] = 0$ .

We propose a novel, yet straightforward strategy to expand data outside of training distributional support: perturb instances to lie further away from the origin in latent space. In particular, if we have latent vector  $z = \varphi(x)$ , we propose to consider perturbations of the form  $z' = (1 + |\epsilon|)z$  where

<sup>2</sup>We avoid any modality or domain-specific augmentations.

$\epsilon \sim \mathcal{N}(0, \sigma^2)$ , and one can utilize the decoder  $x' = \gamma(z')$ . I.e., we define our expansion operation on a set of points as:

$$\mathbf{Ex}(\{x_i\}_{i=1}^N) \equiv \{\gamma((1 + |\epsilon_i|)\varphi(x_i)) \mid \epsilon_i \sim \mathcal{N}(0, \sigma^2)\}_{i=1}^N. \quad (2)$$

**Ex** will be a *stochastic* mapping. As shown in Fig. 3, our expansion covers areas away from the training support, even covering areas of OOD data. However, unlike with small jitter-based perturbations, where one can retain an original instance label, it is less clear how to derive an accompanying training signal for expansive augmentations. Below, we propose to leverage a pseudo-labeling scheme where we derive  $K$  labels with the base experts ( $f_1(x'), \dots, f_K(x')$ )<sup>3</sup>.

### 3.3 EMOE: Expansive Matching of Experts

Once we generate extrapolated data via latent expansion, the key challenge becomes how to provide supervision on these OOD samples. Since true labels are unavailable, we leverage predictions from base experts to pseudo label these points. To retain the diversity in the base experts, we propose a multi-headed neural architecture trained via self-training. Specifically, the network consists of a shared multilayer perceptron (MLP), denoted as  $\phi : \mathbb{R}^d \rightarrow \mathbb{R}^m$ , which learns a common representation space, and  $K$  expert-specific heads,  $h_1, \dots, h_K$ , where each head maps the shared representation to a prediction, e.g.,  $h_j : \mathbb{R}^m \rightarrow \mathbb{R}$  for binary classification. Importantly, each head is trained to match the output of a different base expert, enabling the model to align with multiple diverse supervisory signals. The training loss is defined as a sum of per-head losses on a pseudo-labeled set  $\mathcal{S}$ , where each  $h_j$  is optimized to match the corresponding expert's predictions. This encourages shared representation to support generalization across diverse pseudo-labeling sources. Our per head loss that matches pseudo labels provided by the experts to the MLP heads on a set  $\mathcal{S}$  is as follows:

$$\mathcal{L}_{\text{match}}(\phi, \{h_j\}_{j=1}^K, \{g_j\}_{j=1}^K; \mathcal{S}) \quad (3)$$

$$\equiv \frac{1}{|\mathcal{S}|K} \sum_{x \in \mathcal{S}} \sum_{j=1}^K \ell(h_j(\phi(x)), g_j(x)), \quad (4)$$

where  $\ell(\hat{y}, y)$  is a supervised loss (e.g., the cross-entropy loss). Moreover, we will utilize a mean-matching L1 loss

$$\mathcal{L}_{\text{mean}}(\phi, \{h_j\}_{j=1}^K, \{g_j\}_{j=1}^K; \mathcal{S}) \quad (5)$$

$$\equiv \frac{1}{|\mathcal{S}|} \sum_{x \in \mathcal{S}} \left\| \frac{1}{K} \sum_{j=1}^K \sigma(h_j(\phi(x))) - \frac{1}{K} \sum_{j=1}^K g_j(x) \right\|_1, \quad (6)$$

where  $\sigma(\cdot)$  is the sigmoid. Our full expansive matching of experts' loss is then:

$$\mathcal{L}_{\text{EMOE}}(\phi, \{h_j\}_{j=1}^K, \{g_j\}_{j=1}^K; \mathcal{D}) \quad (7)$$

$$\equiv \mathcal{L}_{\text{mean}}(\phi, \{h_j\}_{j=1}^K, \{g_j\}_{j=1}^K; \mathcal{D}) \quad (8)$$

$$+ \mathcal{L}_{\text{match}}(\phi, \{h_j\}_{j=1}^K, \{g_j\}_{j=1}^K; \mathcal{D}) \quad (9)$$

$$+ \lambda \mathcal{L}_{\text{match}}(\phi, \{h_j\}_{j=1}^K, \{g_j\}_{j=1}^K; \mathbf{Ex}(\mathcal{D})). \quad (10)$$

<sup>3</sup>One may also train base experts directly on the latent space,  $(f_1(z'), \dots, f_K(z'))$ , and avoid the decoder.

Note that we provide additional supervisory losses on non-augmented  $\mathcal{D}$  via  $\mathcal{L}_{\text{mean}}$ . Empirical results show (§ 4) that the network heads learn often learn a better estimator than the base experts. However, we see more consistent improvements by not discarding the base experts and bagging:

$$f_{\text{EMOE}}(x) \equiv \frac{1}{2K} \sum_{j=1}^K g_j(x) + h_j(\phi(x)). \quad (11)$$

**Motivation** We expound on how EMOE may learn better estimates on OOD data through *diversity and multi-task learning*, and *variance reduction and regularization*.

*Diversity and Multi-task Learning.* In practice, we propose simple linear heads. At an intuitive level, this forces the MLP to learn a robust feature embedding that can ‘mimic’ the diverse views that the base experts provide. That is, this will force the last hidden layer to featureize an embedding  $\phi(x)$  that can, with simple linear projections, emulate a diverse set of labels. The per-head matching loss (4) may be formulated as a multi-task loss on a set  $\mathcal{S}$  of  $K$  virtual environments  $\mathcal{E}_j(\mathcal{S}) = \{(x, g_j(x)) \mid x \in \mathcal{S}\}$ :  $\mathcal{L}_{\text{match}}(\phi, \{h_j\}_{j=1}^K, \{g_j\}_{j=1}^K; \mathcal{S}) = \frac{1}{K} \sum_{j=1}^K \mathcal{L}(h_j(\phi(\cdot)), \mathcal{E}_j(\mathcal{S}))$ , where  $\mathcal{L}(h_j(\phi(\cdot)), \mathcal{E}_j(\mathcal{S}))$  is the supervised loss on instances/labels in environment  $\mathcal{E}_j(\mathcal{S})$  with estimator  $h_j(\phi(\cdot))$  on the shared embedding  $\phi$ . Thus, when training on the expanded set of data-points,  $\mathbf{Ex}(\mathcal{D})$ , with pseudo-labels stemming from diverse experts (e.g., trained on different subsets of features and instances), we see that our matching loss provides supervisory signals to learn: 1) on OOD data (through expansion); 2) robust embeddings that must generalize to diverse environments.

*Variance Reduction and Regularization.* Previous work has decomposed OOD generalization into bias/variance terms (Yang et al. 2020; Arpit et al. 2022b):

$$\mathbb{E}_{(x,y) \sim \mathcal{P}_{\text{out}}} \mathbb{E}_{\mathcal{D} \sim \mathcal{P}_{\text{in}}} [\text{CE}(y, f(x; \mathcal{D}))] \quad (12)$$

$$= \mathbb{E}_{(x,y)} [\text{CE}(y, \bar{f}(x))] + \mathbb{E}_{x, \mathcal{D}} [\text{KL}(\bar{f}(x), f(x; \mathcal{D}))], \quad (13)$$

where  $\text{CE}$  is the cross-entropy loss,  $f(x; \mathcal{T})$  is the model fit on dataset  $\mathcal{T}$ ,  $\bar{f}(x) = \mathbb{E}_{\mathcal{D}}[f(x; \mathcal{D})]$  is the expected prediction when averaging out draws on the (in-distribution) training dataset  $\mathcal{D}$ , and  $\mathcal{P}_{\text{out}}$  is the OOD data distribution at inference time. Letting  $\bar{g}(x) \equiv \frac{1}{K} \sum_{j=1}^K g_j(x)$ , we may view  $\bar{g}(x)$  as a bootstrap-like estimate for  $\bar{f}(x)$ . One may then take  $\mathbb{E}_{x, \mathcal{D}} [\text{KL}(\bar{g}(x), f(x; \mathcal{D}))]$  as a proxy for  $\mathbb{E}_{x, \mathcal{D}} [\text{KL}(\bar{f}(x), f(x; \mathcal{D}))]$  and roughly consider

$$\mathbb{E}_{(x,y) \sim \mathcal{P}_{\text{out}}} \mathbb{E}_{\mathcal{D} \sim \mathcal{P}_{\text{in}}} [\text{CE}(y, f(x; \mathcal{D}))] \quad (14)$$

$$\approx \mathbb{E}_{(x,y)} [\text{CE}(y, \bar{f}(x))] + \mathbb{E}_{x, \mathcal{D}} [\text{KL}(\bar{g}(x), f(x; \mathcal{D}))], \quad (15)$$

which connects to (7) when interpreting our expanded points as a proxy for the (unknown) OOD distribution  $\mathcal{P}_{\text{out}}$  and  $\mathcal{L}_{\text{match}}(\phi, \{h_j\}_{j=1}^K, \{g_j\}_{j=1}^K; \mathbf{Ex}(\mathcal{E}))$  as a proxy for  $\mathbb{E}_{x, \mathcal{D}} [\text{KL}(\bar{g}(x), f(x; \mathcal{D}))]$ .

## 4 Experiments

We conduct experiments on a varied set of real-world datasets to test the OOD generalizability of EMOE. We

Table 1: Experiment results on DrugOOD (Ji et al. 2023) datasets. We **bold** best scores based on the mean minus 1 standard error. We *italicize* best scores when they are achieved by a semi-supervised method (\*), that uses additional unlabeled OOD data during training.

		refined ec50 val	refined ec50 test	core ic50 val	core ic50 test	core ec50 val	core ec50 test
AUPRC@ R<0.2	DivDis*	96.02±0.19	86.51±0.28	97.80±0.07	89.72±0.06	93.86±0.42	80.18±0.92
	FixMatch*	94.48±0.47	86.38±0.35	97.62±0.06	92.89±1.36	95.02±0.76	70.49±0.43
	D-BAT	96.97±0.16	88.78±0.40	98.13±0.08	91.79±0.38	93.81±0.22	<b>84.35±1.35</b>
	AdvStyle	95.13±0.13	88.21±0.37	97.04±0.17	89.05±0.22	94.84±0.31	84.51±2.36
	EoA	85.03±0.06	78.79±0.14	88.56±0.05	77.03±0.13	81.85±0.24	71.84±0.45
	Mixup	85.39±0.23	79.78±0.34	88.99±0.43	78.07±0.61	83.97±0.61	73.04±0.42
	NCDG	93.92±0.62	84.46±0.67	97.83±0.08	87.82±0.26	93.40±0.78	80.09±1.94
	EMOE base	98.00±0.07	89.48±0.24	<b>99.14±0.02</b>	94.20±0.15	97.79±0.11	68.48±0.30
	EMOE	<b>98.45±0.06</b>	<b>89.76±0.26</b>	99.15±0.05	<b>94.42±0.09</b>	<b>98.66±0.10</b>	69.04±0.50
AUPRC	DivDis*	89.62±0.12	80.92±0.06	93.34±0.10	81.48±0.30	83.85±0.41	75.09±0.38
	FixMatch*	87.14±0.58	81.51±0.31	92.38±0.15	82.78±0.57	80.92±1.12	70.57±0.32
	D-BAT	84.70±0.51	70.08±0.69	90.84±0.28	73.45±0.90	76.64±0.49	54.87±0.99
	AdvStyle	83.01±0.90	69.48±2.16	88.54±1.44	72.11±1.49	81.17±1.72	58.40±2.18
	EoA	69.66±0.47	57.71±0.79	79.12±0.09	56.52±0.42	64.16±0.51	36.50±1.48
	Mixup	80.36±0.88	72.88±1.67	86.88±0.14	74.99±0.15	73.03±1.67	60.84±4.31
	NCDG	89.27±0.22	80.54±0.21	94.17±0.08	81.19±0.11	87.72±0.37	74.99±0.74
	EMOE base	91.21±0.02	82.61±0.05	94.91±0.03	84.13±0.06	88.44±0.05	<b>71.80±0.07</b>
	EMOE	<b>91.59±0.03</b>	<b>83.06±0.10</b>	<b>95.38±0.01</b>	<b>87.77±0.02</b>	<b>89.52±0.05</b>	71.41±0.11

considered the single source domain generalization setting (e.g., (Qiao, Zhao, and Peng 2020)), where our model is trained solely on ID data without any (labeled or unlabeled) OOD data during training/validation (e.g., precluding typical semi-supervised approaches), and without any accompanying environmental/domain/source information from ID training instances. Moreover, we note that we avoided utilizing any modality-specific information in EMOE (e.g., we do not utilize any domain specific augmentations) for generality. We utilized XGB Classifiers (Chen and Guestrin 2016) fitted to random subsets of data instances and features as the base collection of experts. For a fair/realistic evaluation, we avoided any hyper-parameter tuning on EMOE and utilized a fixed architecture of a 2 layer 512 ELU (Clevert, Unterthiner, and Hochreiter 2015) hidden-unit MLP with 1024 linear-output heads (please see other hyperparameters in Appx.A.1). For our latent space, we utilize PCA with 128 components. While OOD generalization is an active field of research (Freiesleben and Grote 2023; Liu et al. 2021), methodology for general (non-modality specific) single source domain generalization is more limited. We provide context to our results through comparisons to a diverse set of existing strong domain generalization methods that approach the problem from various perspectives (and are applicable in the single-source setting).

**Single-Source Baselines** In our experiments, we include three baselines that utilize data augmentation: AdvStyle (Zhong et al. 2022), Mixup (Zhang et al. 2018), and NCDG (Tian et al. 2022) as well as two baselines employing ensemble methods: D-BAT (Pagliardini et al. 2023) and EoA (Arpit et al. 2022a). Mixup linearly combines two ID samples, AdvStyle adversarially augments ID data, NCDG takes a simple augmentation and optimizes neuron coverage, D-BAT enforces prediction diversity on OOD data, and EoA ensembles moving average models.

**Semi-Supervised Baselines** We provide further context by comparing to semi-supervised methods for general tabular data, DivDis (Lee, Yao, and Finn 2022) and

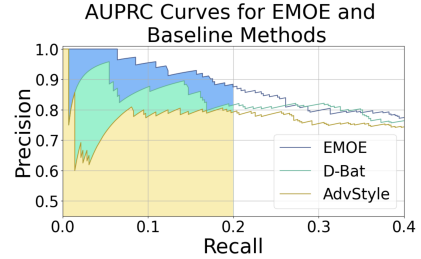


Figure 4: AUPRC at recall < 0.2 for EMOE and competitive baselines on hERG dataset.

FixMatch (Sohn et al. 2020). Note, these methods utilize more information than EMOE, and *have access to unlabeled OOD data from the test-time distribution*. That is, these approaches break from our single-source generalization setting and utilize additional information of the test-time distribution. DivDis is a two-stage framework that first trains diverse model heads using unlabeled target OOD data and then selects the best head with minimal supervision (i.e., using a single label from target OOD data). FixMatch generates filtered pseudo-labels using the model’s predictions on weakly-augmented OOD unlabeled samples. The model is then trained to predict the pseudo-label when provided with a strongly augmented version of the same sample. As DivDis and FixMatch utilize additional information from single-source methods, we separate their results and denote them with an asterisk\*.

**Metrics** For prediction thresholding (rejection), we directly utilize the conditional probability  $P(Y = 1 | X = x)$  generated by the models. Many real-world applications (e.g. drug virtual screening) utilize only high-confidence predictions. Thus, we paid close attention to high-confidence filtration and reported percent of AUPRC at conservative recall thresholds ‘AUPRC@R<7’ (see Eq.1 for formal definition and Fig.4 for illustration). We also reported AUPRC, AUROC (see Appx. B.1 & B.2 for results on AUROC, which

follow a similar trend) We report both base expert (‘EMOE Base’) and EMOE (Eq.11) ensemble performance. Our code will be open-sourced upon publication.

Table 2: Experiment results on ChEMBL (Gaulton et al. 2011) and Therapeutics Data Commons (Huang et al. 2021) datasets. We **bold** best scores based on the mean minus standard error.

		hERG	A549_cells	cyp_2D6	Ames
AUPRC@ R<0.2	DivDis*	85.65 $\pm$ 0.37	89.45 $\pm$ 1.16	79.98 $\pm$ 1.10	95.80 $\pm$ 0.34
	FixMatch*	79.66 $\pm$ 0.57	90.81 $\pm$ 4.30	83.58 $\pm$ 1.98	93.55 $\pm$ 0.64
	D-BAT	84.48 $\pm$ 1.74	98.26 $\pm$ 0.14	91.40 $\pm$ 0.98	99.04 $\pm$ 0.24
	AdvStyle	88.21 $\pm$ 0.77	97.77 $\pm$ 0.28	84.83 $\pm$ 0.93	<b>99.05<math>\pm</math>0.17</b>
	EoA	63.80 $\pm$ 0.42	61.31 $\pm$ 0.31	61.77 $\pm$ 0.41	78.74 $\pm$ 0.43
	Mixup	82.25 $\pm$ 1.51	95.04 $\pm$ 0.25	87.09 $\pm$ 2.32	91.02 $\pm$ 1.06
	NCDG	78.25 $\pm$ 2.60	90.33 $\pm$ 0.95	79.31 $\pm$ 2.44	87.86 $\pm$ 1.41
	EMOE base	94.44 $\pm$ 0.17	98.22 $\pm$ 0.08	95.51 $\pm$ 0.19	97.84 $\pm$ 0.20
	EMOE	<b>94.67<math>\pm</math>0.29</b>	<b>98.87<math>\pm</math>0.09</b>	<b>96.88<math>\pm</math>0.25</b>	98.45 $\pm$ 0.19
AUPRC	DivDis*	67.70 $\pm$ 0.25	76.45 $\pm$ 0.63	65.76 $\pm$ 0.45	82.37 $\pm$ 0.27
	FixMatch*	45.16 $\pm$ 3.11	51.31 $\pm$ 1.28	32.65 $\pm$ 2.16	72.54 $\pm$ 1.15
	D-BAT	54.60 $\pm$ 1.59	67.04 $\pm$ 0.53	47.42 $\pm$ 0.85	70.44 $\pm$ 0.76
	AdvStyle	51.54 $\pm$ 0.93	65.02 $\pm$ 0.72	44.41 $\pm$ 0.96	74.98 $\pm$ 0.49
	EoA	43.30 $\pm$ 0.51	44.95 $\pm$ 0.24	37.37 $\pm$ 0.95	59.43 $\pm$ 0.18
	Mixup	42.42 $\pm$ 0.85	50.52 $\pm$ 0.50	27.79 $\pm$ 1.49	60.94 $\pm$ 0.80
	NCDG	65.03 $\pm$ 0.75	79.50 $\pm$ 0.79	65.31 $\pm$ 1.00	76.48 $\pm$ 0.30
	EMOE base	72.19 $\pm$ 0.07	84.10 $\pm$ 0.01	72.93 $\pm$ 0.13	87.43 $\pm$ 0.02
	EMOE	<b>73.26<math>\pm</math>0.08</b>	<b>84.60<math>\pm</math>0.08</b>	<b>73.59<math>\pm</math>0.15</b>	<b>88.50<math>\pm</math>0.10</b>

## 4.1 Chemical Datasets

To test how well EMOE generalizes to OOD data in chemical domains, we considered seven datasets from ChEMBL (Gaulton et al. 2011), Therapeutics Data Commons (Huang et al. 2021), and DrugOOD (Ji et al. 2023). For all datasets, we represented molecules using extended-connectivity fingerprints (Rogers and Hahn 2010) with radius 2 (ECFP4) and with dimensionality 1024. ECFP4 is a standard method for molecular representation and was chosen for its simplicity in calculation as well as its ability to perform comparably to learned representations, such as those generated by graph neural networks on relevant classification tasks (Zagidullin et al. 2021). Datasets for inhibition of human Ether-à-go-go-Related Gene (hERG), cytotoxicity of human A549 cells (A549\_cells), and agonists for Cytochrome P450 2D6 (cyp\_2D6) were collected from ChEMBL (Gaulton et al. 2011). For these datasets, binary classification labels were generated with a pChEMBL threshold of 5.0. We also considered another binary classification dataset for Ames mutagenicity (Ames) that was taken from Therapeutics Data Commons (TDC) (Huang et al. 2021). For the ChEMBL and TDC datasets (hERG, A549\_cells, cyp\_2D6, and Ames), ID and OOD splits were determined based on the Murko scaffold of a molecule, such that OOD data have molecular scaffolds not present in the ID data, mimicking the “scaffold domain” approach utilized in DrugOOD (Ji et al. 2023).

Moreover, we considered the “core ec50,” “refined ec50,” and “core ic50” ligand-based affinity prediction datasets (lbap) from DrugOOD (Ji et al. 2023) (the three hardest OOD performance gap datasets). For these datasets ID and OOD splits were determined based on the number of atoms in a molecule, such that larger molecules are considered the OOD set and smaller molecules, the ID set. Datasets are or-

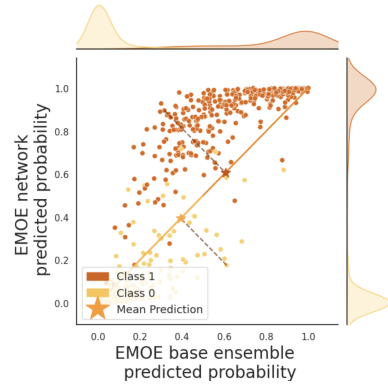


Figure 5: *Predicted probabilities from EMOE network and base experts.* We highlight example instances where the base experts initially makes incorrect predictions but are corrected when we average the predicted probabilities from EMOE network and EMOE base.

ganized by domain and subsequently divided into training, OOD validation, and OOD testing sets in sequential order. While larger in samples, the DrugOOD datasets ignore the impact of biological targets on label, resulting in a modeling task that has limited relevance to drug discovery. The additional ChEMBL/TDC datasets, though smaller, have direct relevance for drug discovery.

**Results** We assessed models on ChEMBL, TDC, and DrugOOD datasets; our results are shown in Tab. 2 and Tab. 1. Across the chemical datasets, EMOE consistently outperforms both supervised and semi-supervised baselines and consistently shows gains over its base experts. Note further, that EMOE’s performance gain is especially impactful at conservative recalls (AUPRC@R<0.2, e.g., see Fig. 4), which indicates the EMOE outperform other models in virtual screening tasks to filter drug candidates (where false positives would lead to wasted resources). Please see discussion below (§ 4.4), for further analysis on the improved performance of EMOE w.r.t. increased confidence (Fig. 5) and expert diversity (Fig. 6).

## 4.2 Other Real World Datasets

Next, we further evaluate our method in non-chemical domains across a diverse range of real-world OOD scenarios using the Tableshift datasets (Gardner, Popovic, and Schmidt 2023) (and the PACS image dataset (Li et al. 2017), see Mat. B.5). We selected a diverse collection of Tableshift datasets, based on unrestricted availability and in/out-of-domain performance discrepancy, coverings areas including: finance, education, and healthcare. Each dataset has an associated real-world shift and a related prediction target (see Gardner, Popovic, and Schmidt (2023) for further details). Results on the Tableshift are shown in Tab. 8. As before, we consider the same single-source domain generalization setting. We can see that even over diverse applications, our EMOE method is able to perform well and is often outperforming our strong competing baselines. Moreover, even though DivDis and FixMatch use additional unla-

Table 3: Experiment results on Tableshift (Gardner, Popovic, and Schmidt 2023) datasets. We **bold** best scores based on the mean minus 1 standard error.

		Childhood Lead	FICO HELOC	Hospital Readmission	Sepsis
AUPRC@ R<0.2	DivDis*	89.77 $\pm$ 2.51	85.50 $\pm$ 2.65	83.22 $\pm$ 2.57	60.66 $\pm$ 1.57
	FixMatch*	81.75 $\pm$ 3.69	77.76 $\pm$ 1.94	67.84 $\pm$ 1.95	17.28 $\pm$ 0.58
	D-BAT	62.82 $\pm$ 0.00	91.20 $\pm$ 0.24	<b>78.84<math>\pm</math>0.12</b>	75.37 $\pm$ 0.38
	AdvStyle	64.96 $\pm$ 0.01	88.71 $\pm$ 0.65	72.91 $\pm$ 0.58	59.83 $\pm$ 0.63
	EoA	77.43 $\pm$ 0.97	59.53 $\pm$ 2.24	51.83 $\pm$ 1.66	41.10 $\pm$ 1.56
	Mixup	50.00 $\pm$ 0.00	91.16 $\pm$ 2.10	69.19 $\pm$ 3.95	66.09 $\pm$ 1.15
	NCDG	42.49 $\pm$ 1.31	87.93 $\pm$ 2.35	68.88 $\pm$ 1.15	15.22 $\pm$ 0.38
	EMOE base	97.39 $\pm$ 0.06	90.07 $\pm$ 0.32	58.30 $\pm$ 0.09	<b>78.62<math>\pm</math>1.57</b>
	EMOE	<b>97.92<math>\pm</math>0.20</b>	<b>91.72<math>\pm</math>0.62</b>	67.57 $\pm$ 0.12	76.95 $\pm$ 1.45
AUPRC	DivDis*	76.33 $\pm$ 0.86	82.47 $\pm$ 1.05	65.95 $\pm$ 2.15	58.85 $\pm$ 1.21
	FixMatch*	75.39 $\pm$ 0.58	72.22 $\pm$ 4.46	56.54 $\pm$ 1.21	18.24 $\pm$ 0.66
	D-BAT	71.85 $\pm$ 0.01	80.91 $\pm$ 0.17	63.29 $\pm$ 0.08	58.17 $\pm$ 0.21
	AdvStyle	48.37 $\pm$ 2.77	79.63 $\pm$ 1.65	38.13 $\pm$ 3.80	54.34 $\pm$ 0.27
	EoA	49.48 $\pm$ 0.19	59.53 $\pm$ 2.24	29.45 $\pm$ 4.95	11.21 $\pm$ 2.21
	Mixup	50.00 $\pm$ 0.00	80.95 $\pm$ 0.63	14.15 $\pm$ 1.06	56.80 $\pm$ 0.40
	NCDG	23.08 $\pm$ 0.24	79.05 $\pm$ 1.21	58.95 $\pm$ 0.23	11.96 $\pm$ 0.32
	EMOE base	86.39 $\pm$ 0.19	83.80 $\pm$ 0.07	62.83 $\pm$ 0.03	<b>64.01<math>\pm</math>0.94</b>
	EMOE	<b>86.70<math>\pm</math>0.28</b>	<b>84.02<math>\pm</math>0.09</b>	<b>63.62<math>\pm</math>0.08</b>	62.21 $\pm$ 0.52

beled OOD data, EMOE outperforms both on the majority of datasets, highlighting EMOE’s ability for generalization on completely *unforeseen* OOD instances (without any knowledge of test time distribution).

### 4.3 Ablation Studies

**Model Agnostic Property** Despite its dependency on base

Table 4: ChEMBL Datasets’ Mean @R<0.2 Ablating Type of Base Experts.

	XGBoost	Random Forest	Decision Tree	D-BAT
Base	95.87	95.72	92.18	91.63
EMOE	<b>96.64</b>	<b>96.15</b>	<b>94.15</b>	<b>93.81</b>

experts for pseudo-label generation, EMOE consistently improves performance across a wide range of base model types, including XGBoost, Random Forest, Decision Tree, and the OOD generalization method D-BAT (Pagliardini et al. 2023). As shown in Tab.4 (see details on this ablation in Appx.B.6). EMOE consistently improves upon each kind of base model, demonstrating its effectiveness as a model-agnostic framework. Moreover, this shows the future promise of *incorporating EMOE with complementary methodology for OOD generalizability*.

**Per-head Matching Ablation** Next, we ablate on the per-expert matching loss scheme (eq.7) used in EMOE with a simpler alternative: mean-only matching (MM) (eq.8) on the expanded points. This ablation tests whether the diversity induced by per-head supervision aids performance. Here we utilized single headed (SH) and multi-headed (MH) MLPs with mean matching, where EMOE uses multi-headed MLP with per expert loss (see Mat.B.7 for details on the alternative losses). EMOE achieves the highest AUPRC improvements ( $\Delta$ ) over base experts (+1.11 at R<.2, +1.03 at R<1) compared to SH+MM (+0.59, +0.45) and MH+MM (+0.25, +0.55), showing evidence for the effectiveness of training

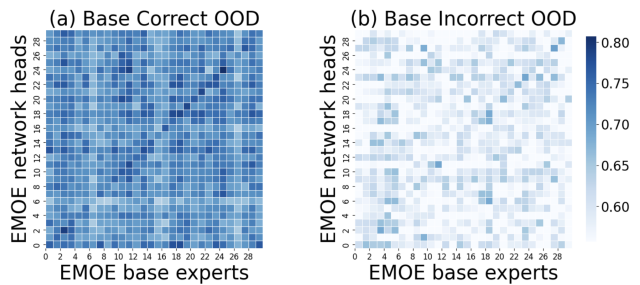


Figure 6: Experts correlations between EMOE base experts and EMOE network heads on “Ames” dataset. (a) EMOE experts have a high correlation with EMOE base experts on sample the base experts make correct predictions. (b) EMOE experts show low correlations with EMOE base experts on samples where the base experts make incorrect predictions.

our embedding through the diverse multi-task loss induced by per-head matching (§ 3).

**Bottleneck Ablation** We motivated EMOE’s performance in terms of a multi-task scheme, which bottlenecks (the last hidden layer) to learn an embedding that can generalize to mimic predictions on a diverse set of pseudo-labels (§ 3). We test this motivation by comparing the original architecture (Full:  $2 \times 512$  hidden layer) with a stronger bottleneck still, a small architecture (Tiny:  $2 \times 32$  hidden layer). (See Appx. B.8 for more details and results.) The performance gap is marginal between the ‘Full’ and ‘Tiny’ model (a 0.85% difference) when using our proposed loss. In contrast, when using empirical risk minimization, we see a 4.87 times bigger drop in performance between ‘Full’ and ‘Tiny’ models. This suggests that the bottlenecking properties of our method are key to EMOE’s performance, and show promise for EMOE in resource-constrained settings.

### 4.4 Discussion

EMOE addresses the challenging single source OOD generalization problem for real-valued vector data, outperforming baselines, including those that leverage unlabelled OOD data. Across all metrics/datasets, EMOE achieves leading tally of 29, far exceeding both EMOE base and the next highest score of 4 from the strong competing baseline D-Bat (Pagliardini et al. 2023) as shown in Fig. 1. Despite its performance, EMOE does not incur an out-sized computational cost; the training of base experts may be done in parallel, and the cost of expanding data in the latent space is negligible (see Appx. A.3 for addition timing details).

In summary, EMOE presents a simple yet powerful model-agnostic approach to OOD generalization under single-source setting via pseudo-labels and expert-specific matching. EMOE’s architecture promotes a robust embedding and stands out in high confidence areas for OOD predictions. We believe this work opens promising directions for general-purpose, modality- and model- agnostic OOD learning, particularly in high-stakes applications like drug discovery, where confident extrapolation is critical and labeled data is scarce.

## References

Arjovsky, M.; Bottou, L.; Gulrajani, I.; and Lopez-Paz, D. 2019. Invariant Risk Minimization. *ArXiv*, abs/1907.02893.

Arpit, D.; Wang, H.; Zhou, Y.; and Xiong, C. 2022a. Ensemble of Averages: Improving Model Selection and Boosting Performance in Domain Generalization. In *Advances in Neural Information Processing Systems*.

Arpit, D.; Wang, H.; Zhou, Y.; and Xiong, C. 2022b. Ensemble of averages: Improving model selection and boosting performance in domain generalization. *Advances in Neural Information Processing Systems*, 35: 8265–8277.

Berthelot, D.; Carlini, N.; Cubuk, E. D.; Kurakin, A.; Sohn, K.; Zhang, H.; and Raffel, C. 2020. ReMixMatch: Semi-Supervised Learning with Distribution Matching and Augmentation Anchoring. In *International Conference on Learning Representations*.

Cascante-Bonilla, P.; Tan, F.; Qi, Y.; and Ordonez, V. 2020. Curriculum Labeling: Revisiting Pseudo-Labeling for Semi-Supervised Learning. In *AAAI Conference on Artificial Intelligence*.

Chen, T.; and Guestrin, C. 2016. XGBoost: A Scalable Tree Boosting System. *Proceedings of the 22nd ACM SIGKDD International Conference on Knowledge Discovery and Data Mining*.

Cheung, T.-H.; and Yeung, D.-Y. 2021. MODALS: Modality-agnostic Automated Data Augmentation in the Latent Space. In *International Conference on Learning Representations*.

Clevert, D.-A.; Unterthiner, T.; and Hochreiter, S. 2015. Fast and Accurate Deep Network Learning by Exponential Linear Units (ELUs). *arXiv: Learning*.

Cubuk, E. D.; Zoph, B.; Shlens, J.; and Le, Q. V. 2019. RandAugment: Practical automated data augmentation with a reduced search space. *2020 IEEE/CVF Conference on Computer Vision and Pattern Recognition Workshops (CVPRW)*, 3008–3017.

Devries, T.; and Taylor, G. W. 2018. Learning Confidence for Out-of-Distribution Detection in Neural Networks. *ArXiv*, abs/1802.04865.

Dietterich, T. G. 2007. Ensemble Methods in Machine Learning.

Ding, Y.; Wang, L.; Liang, B.; Liang, S.; Wang, Y.; and Chen, F. 2022. Domain Generalization by Learning and Removing Domain-specific Features. *ArXiv*, abs/2212.07101.

Dou, Q.; de Castro, D. C.; Kamnitsas, K.; and Glocker, B. 2019. Domain Generalization via Model-Agnostic Learning of Semantic Features. In *Neural Information Processing Systems*.

Dubuisson, B.; and Masson, M. 1993. A statistical decision rule with incomplete knowledge about classes. *Pattern Recognit.*, 26: 155–165.

Eigen, D.; Ranzato, M.; and Sutskever, I. 2013. Learning Factored Representations in a Deep Mixture of Experts. *CoRR*, abs/1312.4314.

Freiesleben, T.; and Grote, T. 2023. Beyond generalization: a theory of robustness in machine learning. *Synthese*, 202(4): 109.

Fumera, G.; Roli, F.; and Giacinto, G. 2000. Reject option with multiple thresholds. *Pattern Recognit.*, 33: 2099–2101.

Gardner, J.; Popovic, Z.; and Schmidt, L. 2023. Benchmarking Distribution Shift in Tabular Data with TableShift. *Advances in Neural Information Processing Systems*.

Gaulton, A.; Bellis, L. J.; Bento, A. P.; Chambers, J.; Davies, M.; Hersey, A.; Light, Y.; McGlinchey, S.; Michalovich, D.; Al-Lazikani, B.; and Overington, J. P. 2011. ChEMBL: a large-scale bioactivity database for drug discovery. *Nucleic Acids Research*, 40: D1100 – D1107.

Geifman, Y.; and El-Yaniv, R. 2017. Selective Classification for Deep Neural Networks. *ArXiv*, abs/1705.08500.

Geifman, Y.; and El-Yaniv, R. 2019. SelectiveNet: A Deep Neural Network with an Integrated Reject Option. In *International Conference on Machine Learning*.

Ghosh, S.; Kumar, S.; Verma, J.; and Kumar, A. 2021. Self Training with Ensemble of Teacher Models. *ArXiv*, abs/2107.08211.

Hendrickx, K.; Perini, L.; Van der Plas, D.; Meert, W.; and Davis, J. 2024. Machine learning with a reject option: A survey. *Machine Learning*, 1–38.

Hu, Y.; Stumpfe, D.; and Bajorath, J. 2017. Recent advances in scaffold hopping: miniperspective. *Journal of medicinal chemistry*, 60(4): 1238–1246.

Huang, K.; Fu, T.; Gao, W.; Zhao, Y.; Roohani, Y.; Leskovec, J.; Coley, C. W.; Xiao, C.; Sun, J.; and Zitnik, M. 2021. Therapeutics Data Commons: Machine Learning Datasets and Tasks for Drug Discovery and Development. *arXiv:2102.09548*.

Jang, H.; Tack, J.; Choi, D.; Jeong, J.; and Shin, J. 2023. Modality-Agnostic Self-Supervised Learning with Meta-Learned Masked Auto-Encoder. *ArXiv*, abs/2310.16318.

Ji, Y.; Zhang, L.; Wu, J.; Wu, B.; Li, L.; Huang, L.-K.; Xu, T.; Rong, Y.; Ren, J.; Xue, D.; et al. 2023. Drugood: Out-of-distribution dataset curator and benchmark for ai-aided drug discovery—a focus on affinity prediction problems with noise annotations. In *Proceedings of the AAAI Conference on Artificial Intelligence*, volume 37, 8023–8031.

Jordan, M. I.; and Jacobs, R. A. 1993. Hierarchical Mixtures of Experts and the EM Algorithm. *Neural Computation*, 6: 181–214.

Kingma, D. P.; and Ba, J. 2014. Adam: A Method for Stochastic Optimization. *CoRR*, abs/1412.6980.

Koyama, M.; and Yamaguchi, S. 2020. Out-of-Distribution Generalization with Maximal Invariant Predictor. *ArXiv*, abs/2008.01883.

Kussul, E. M.; Makeyev, O.; Baidyk, T.; and Reyes, D. C. 2010. Neural network with ensembles. *The 2010 International Joint Conference on Neural Networks (IJCNN)*, 1–7.

Lee, D.-H. 2013. Pseudo-Label : The Simple and Efficient Semi-Supervised Learning Method for Deep Neural Networks.

Lee, S.; Yin, C.; and Zhang, P. 2023. Stable clinical risk prediction against distribution shift in electronic health records. *Patterns*, 4.

Lee, Y.; Yao, H.; and Finn, C. 2022. Diversify and disambiguate: Learning from underspecified data. *arXiv preprint arXiv:2202.03418*.

Li, D.; Yang, Y.; Song, Y.-Z.; and Hospedales, T. M. 2017. Deeper, Broader and Artier Domain Generalization. *2017 IEEE International Conference on Computer Vision (ICCV)*, 5543–5551.

Li, Y.; Gong, M.; Tian, X.; Liu, T.; and Tao, D. 2018. Domain Generalization via Conditional Invariant Representations. In *AAAI Conference on Artificial Intelligence*.

Liu, J.; Shen, Z.; He, Y.; Zhang, X.; Xu, R.; Yu, H.; and Cui, P. 2021. Towards out-of-distribution generalization: A survey. *arXiv preprint arXiv:2108.13624*.

Maas, A. L. 2013. Rectifier Nonlinearities Improve Neural Network Acoustic Models.

Pagliardini, M.; Jaggi, M.; Fleuret, F.; and Karimireddy, S. P. 2023. Agree to Disagree: Diversity through Disagreement for Better Transferability. In *The Eleventh International Conference on Learning Representations*.

Qiao, F.; Zhao, L.; and Peng, X. 2020. Learning to Learn Single Domain Generalization. *2020 IEEE/CVF Conference on Computer Vision and Pattern Recognition (CVPR)*, 12553–12562.

Qu, S.; Pan, Y.; Chen, G.-S.; Yao, T.; Jiang, C.; and Mei, T. 2023. Modality-Agnostic Debiasing for Single Domain Generalization. *2023 IEEE/CVF Conference on Computer Vision and Pattern Recognition (CVPR)*, 24142–24151.

Rogers, D.; and Hahn, M. 2010. Extended-Connectivity Fingerprints. *Journal of Chemical Information and Modeling*, 50(5): 742–754. PMID: 20426451.

Serrano, D. R.; Luciano, F. C.; Anaya, B. J.; Ongoren, B.; Kara, A.; Molina, G.; Ramirez, B. I.; Sánchez-Guirales, S. A.; Simon, J. A.; Tomietto, G.; Rapti, C.; Ruiz, H. K.; Rawat, S.; Kumar, D.; and Lalatsa, A. 2024. Artificial Intelligence (AI) Applications in Drug Discovery and Drug Delivery: Revolutionizing Personalized Medicine. *Pharmaceutics*, 16.

Sohn, K.; Berthelot, D.; Carlini, N.; Zhang, Z.; Zhang, H.; Raffel, C. A.; Cubuk, E. D.; Kurakin, A.; and Li, C.-L. 2020. Fixmatch: Simplifying semi-supervised learning with consistency and confidence. *Advances in neural information processing systems*, 33: 596–608.

Srivastava, N.; Hinton, G. E.; Krizhevsky, A.; Sutskever, I.; and Salakhutdinov, R. 2014. Dropout: a simple way to prevent neural networks from overfitting. *J. Mach. Learn. Res.*, 15: 1929–1958.

Stefano, C. D.; Sansone, C.; and Vento, M. 2000. To reject or not to reject: that is the question—an answer in case of neural classifiers. *IEEE Trans. Syst. Man Cybern. Part C*, 30: 84–94.

Thulasidasan, S.; Bhattacharya, T.; Bilmes, J. A.; Chennupati, G.; and Mohd-Yusof, J. 2019. Combating Label Noise in Deep Learning Using Abstention. In *International Conference on Machine Learning*.

Tian, C. X.; Li, H.; Xie, X.; Liu, Y.; and Wang, S. 2022. Neuron coverage-guided domain generalization. *IEEE Transactions on Pattern Analysis and Machine Intelligence*, 45(1): 1302–1311.

Torralba, A.; and Efros, A. A. 2011. Unbiased look at dataset bias. *CVPR 2011*, 1521–1528.

Xie, Q.; Hovy, E. H.; Luong, M.-T.; and Le, Q. V. 2019. Self-Training With Noisy Student Improves ImageNet Classification. *2020 IEEE/CVF Conference on Computer Vision and Pattern Recognition (CVPR)*, 10684–10695.

Yang, Z.; Yu, Y.; You, C.; Steinhardt, J.; and Ma, Y. 2020. Rethinking bias-variance trade-off for generalization of neural networks. In *International Conference on Machine Learning*, 10767–10777. PMLR.

Yao, H.; Yang, X.; Pan, X.; Liu, S.; Koh, P. W.; and Finn, C. 2023. Improving Domain Generalization with Domain Relations.

Yun, S.; Han, D.; Oh, S. J.; Chun, S.; Choe, J.; and Yoo, Y. J. 2019. CutMix: Regularization Strategy to Train Strong Classifiers With Localizable Features. *2019 IEEE/CVF International Conference on Computer Vision (ICCV)*, 6022–6031.

Zagidullin, B.; Wang, Z.; Guan, Y.; Pitkänen, E.; and Tang, J. 2021. Comparative analysis of molecular fingerprints in prediction of drug combination effects. *Briefings in Bioinformatics*, 22(6): bbab291.

Zhang, B.; Wang, Y.; Hou, W.; Wu, H.; Wang, J.; Okumura, M.; and Shinozaki, T. 2021. FlexMatch: Boosting Semi-Supervised Learning with Curriculum Pseudo Labeling. In *Neural Information Processing Systems*.

Zhang, H.; Cisse, M.; Dauphin, Y. N.; and Lopez-Paz, D. 2018. mixup: Beyond Empirical Risk Minimization. In *International Conference on Learning Representations*.

Zhong, Z.; Zhao, Y.; Lee, G. H.; and Sebe, N. 2022. Adversarial style augmentation for domain generalized urban-scene segmentation. *Advances in Neural Information Processing Systems*, 35: 338–350.

Ziyin, L.; Wang, Z. T.; Liang, P. P.; Salakhutdinov, R.; Morency, L.-P.; and Ueda, M. 2019. Deep Gamblers: Learning to Abstain with Portfolio Theory. In *Neural Information Processing Systems*.

Zou, Y.; Yu, Z.; Kumar, B. V. K. V.; and Wang, J. 2018. Unsupervised Domain Adaptation for Semantic Segmentation via Class-Balanced Self-training. In *European Conference on Computer Vision*.

## A Additional Experiment Details

### A.1 EMOE training details

In all of our experiments we used the Adam (Kingma and Ba 2014) optimizer and mini-batches of size 256. One Nvidia A100 GPU with 40GB GPU memory was used to run our experiments, and duration for model training is approximately 0.5 hours.  $\lambda = 0.5$  was used for the  $\mathcal{L}_{\text{match}}$  for the expanded points. As noted in Sec. 3.2 we trained the EMOE models directly in the latent space to avoid the need for the decoder (and also allowed baselines to do this if it aided their performance). In the experiments on hERG, A549\\_cells, CYP\\_2D6, Ames, core ec50, refined ec50, EMOE was trained for 20000 iterations. Arithmetic mean between EMOE and EMOE base was reported. We performed 5 trials on each of the datasets for EMOE.

### A.2 Baseline Setup

We implemented all baselines we are comparing against EMOE following the implementation details in their paper and/or using Github implementations (if available). Since the fingerprints representation of chemicals are quite sparse, we preformed dimension reduction using PCA with 128 components on all chemical datasets. For D-BAT (Pagliardini et al. 2023) with existing implementations designed for tabular data, we utilized their original model architectures. For the other three baseline methods without implementation specifically for tabular data, we adopted a structure comprising two 512 ELU(Clevert, Unterthiner, and Hochreiter 2015) layers to closely mimic the EMOE network architecture. The Adam (Kingma and Ba 2014) optimizer was used for training baseline models.

**D-BAT** In our experiments, the D-Bat(Pagliardini et al. 2023) models used MLP architecture with one 128 LeakyRelu(Maas 2013) layer following the architecture in their Github. Their paper (Pagliardini et al. 2023) discussed two settings, and we focused on the scenario where perturbation data differs from the distribution of test data, adhering to the single-source domain generalization setting. We trained an ensemble of five models sequentially for the D-bat baseline models and the predictions from the 5 models were averaged to obtain the final prediction.

**EoA** We trained an ensemble of 5 simple moving average model following the method described in (Arpit et al. 2022a). We start calculating the moving average at iteration 50 and trained the models for 200 iterations. The predictions from the 5 models were averaged to obtain the final prediction for EoA.

For **AdvStyle** (Zhong et al. 2022) and **Mixup** (Zhang et al. 2018), the methodologies were straightforward. We experimented with training using various numbers of iterations and reported the most promising results. Note that we used alpha=0.7 when combining the 2 samples for Mixup. We executed all baseline experiments five times on each dataset to ensure a precise estimation of performance.

**DivDis** We utilized all unlabeled target OOD data for training and a single label from this data for supervision. An ensemble of 5 models was trained for 100 iterations with early stopping, and each model has 2 classification heads.

Table 5: Training Time for EMOE and baseline methods.

	wall clock (m)
EMOE NN	4.2
Dbat	3.5
EoA	67.9
Advstyle	4.8
Mixup	1.2
NCDG	2.7

Across all datasets, we set  $\lambda_1 = 10$  (encouraging disagreement among model heads), while  $\lambda_2$  (an optional hyperparameter prevents degenerate solutions) was set to 0 for DrugOOD and ChEMBL and to 10 for TableShift. The final prediction is the average of the 5 models’ predictions.

**FixMatch** Originally, Fixmatch (Sohn et al. 2020) was designed for image data, so the sense of weak and strong augmentations were image based. To adapt the method to our modality agnostic setting we used  $x * (1 + \alpha)$  as the weak augmentation,  $x * (1 + 2 * \alpha)$  as strong augmentation, where  $\alpha$  is a small noise drawn from the standard normal distribution.

For **NCDG** (Tian et al. 2022), we adapt the method to use the EMOE architecture (rather than a ResNet model) and the EMOE augmentation method. We set  $t=0.005$  (the threshold for neuron activation in coverage computation),  $\lambda = 0.1$  (the weight coefficient for neuron coverage loss), and  $\beta = 0.01$  (the weight for gradient similarity regularization loss). Five trials were run on each dataset and averaged to obtain the final results.

### A.3 EMOE training time

In Tab. 5, we report the training time for EMOE and baseline models we are considering. Note that the base experts can be training in parallel with enough computational resources (and are each quick to train at < 1s).

## B Additional Experiment and Ablation Results

### B.1 Full Experiment Results on CheMBL and Therapeutics Data Commons

In Tab. 7, we report the full results on hERG, A549\\_cells, cyp\\_2D6, and Ames.

### B.2 Full Experiment Results on DrugOOD

In Tab. 6, we report the full results on core ec50, refined ec 50, and core ic50 from DrugOOD (Ji et al. 2023).

### B.3 Diversity of Predictions

In drug discovery applications, models should predict on structurally diverse compounds. To assess the diversity of model behavior in high confidence out-of-distribution (OOD) predictions, we examine the average variance of fingerprint features for instances with predicted confidence greater than 0.9 on the 3 ChEMBL datasets (var@p>0.9). Higher variance reflects greater heterogeneity among the

Table 6: Full experiment results on DrugOOD datasets. We **bold** best scores based on the mean minus 1 standard deviation. Note that \* refers to a semi-supervised method.

		core ec50 val	core ec50 test	refined ec50 val	refined ec50 test	core ic50 test	core ic 50 test
AUPRC@ R<0.1	DivDis*	96.21±1.02	82.45±2.93	96.63±0.54	88.87±0.58	98.41±0.26	91.72±1.47
	FixMatch*	96.42±1.06	69.80±0.25	94.78±0.63	86.53±0.25	97.70±0.05	95.89±1.46
	D-BAT	94.04±0.25	<b>86.59±1.42</b>	97.19±0.19	88.93±0.48	98.25±0.09	91.89±0.39
	AdvStyle	95.79±0.20	84.56±2.36	96.37±0.32	88.69±0.43	98.10±0.17	89.39±0.33
	EoA	81.85±0.24	71.84±0.45	85.03±0.06	78.79±0.14	88.56±0.05	77.03±0.13
	Mixup	83.97±0.61	73.03±0.42	85.39±0.23	79.78±0.34	88.99±0.43	78.07±0.61
	NCDG	91.95±0.28	80.38±0.47	96.33±0.07	89.94±0.12	97.36±0.08	89.68±0.05
	EMOE base	98.73±0.14	65.40±0.52	<b>99.00±0.04</b>	<b>92.67±0.33</b>	<b>99.57±0.01</b>	<b>96.93±0.09</b>
AUPRC@ R<0.2	DivDis*	93.86±0.42	80.18±0.92	96.02±0.19	86.51±0.28	97.80±0.07	89.72±0.06
	FixMatch*	95.02±0.76	70.49±0.43	94.48±0.47	86.38±0.35	97.62±0.06	92.89±1.36
	D-BAT	93.81±0.22	<b>84.35±1.35</b>	96.97±0.16	88.78±0.40	98.13±0.08	91.79±0.38
	AdvStyle	94.84±0.31	84.51±2.36	95.13±0.13	88.21±0.37	97.04±0.17	89.05±0.22
	EoA	81.85±0.24	71.84±0.45	85.03±0.06	78.79±0.14	88.56±0.05	77.03±0.13
	Mixup	83.97±0.61	73.04±0.42	85.39±0.23	79.78±0.34	88.99±0.43	78.07±0.61
	NCDG	89.82±0.22	77.94±0.39	95.87±0.05	88.60±0.10	96.42±0.06	87.89±0.04
	EMOE base	97.79±0.11	68.48±0.30	98.00±0.07	89.48±0.24	<b>99.14±0.02</b>	92.31±0.14
AUPRC@ R<0.3	DivDis*	91.89±0.95	78.97±1.66	95.19±0.37	85.12±0.49	97.33±0.16	88.06±1.14
	FixMatch*	93.76±1.11	70.61±0.47	87.14±0.64	85.74±0.42	97.59±0.07	91.02±1.24
	D-BAT	93.73±0.21	<b>81.40±0.89</b>	96.89±0.15	87.77±0.32	98.08±0.08	90.71±0.52
	AdvStyle	94.52±0.37	83.57±0.28	94.71±0.13	88.05±0.36	96.69±0.21	88.93±0.19
	EoA	81.85±0.24	71.84±0.45	85.03±0.06	78.79±0.14	88.56±0.05	77.03±0.13
	Mixup	83.97±0.61	73.06±0.43	85.39±0.23	79.78±0.34	88.99±0.43	78.07±0.61
	NCDG	88.73±0.19	76.05±0.35	95.17±0.04	86.07±0.08	95.89±0.05	86.53±0.03
	EMOE base	96.73±0.10	69.94±0.20	97.17±0.06	87.99±0.18	98.71±0.03	92.32±0.23
AUPRC	DivDis*	83.85±0.41	75.09±0.38	89.62±0.12	80.92±0.06	93.34±0.10	81.48±0.30
	FixMatch*	80.92±1.12	70.57±0.32	87.14±0.58	81.51±0.31	92.38±0.15	82.78±0.57
AUROC	D-BAT	76.64±0.49	54.87±0.99	84.70±0.51	70.08±0.69	90.84±0.28	73.45±0.90
	AdvStyle	81.17±1.72	58.40±2.18	83.01±0.90	69.48±2.16	88.54±1.44	72.11±1.49
	EoA	64.16±0.51	36.50±1.48	69.66±0.47	57.71±0.79	79.12±0.09	56.52±0.42
	Mixup	73.03±1.67	60.84±4.31	80.36±0.88	72.88±1.67	86.88±0.14	74.99±0.15
	NCDG	72.74±0.05	55.40±0.20	83.09±0.03	70.63±0.17	89.91±0.03	69.14±0.05
	EMOE base	88.44±0.05	<b>71.80±0.07</b>	91.21±0.02	82.61±0.05	94.91±0.03	84.13±0.06
	EMOE	<b>89.52±0.05</b>	71.41±0.11	<b>91.59±0.03</b>	<b>83.06±0.10</b>	<b>95.38±0.01</b>	<b>84.77±0.02</b>
	DivDis*	65.41±0.81	58.53±0.46	66.68±0.28	57.04±0.08	73.23±0.40	61.15±0.50
AUROC	FixMatch*	70.32±0.59	52.69±0.69	66.37±0.50	58.37±0.58	74.38±0.16	62.05±0.55
	D-BAT	75.26±0.28	58.21±0.26	<b>72.09±0.19</b>	60.32±0.25	<b>80.31±0.08</b>	64.82±0.18
	AdvStyle	75.97±0.39	<b>58.86±0.25</b>	70.78±0.35	59.62±0.30	78.36±0.23	64.14±0.27
	EoA	64.91±0.34	52.71±0.44	59.27±0.20	54.63±0.24	62.99±0.16	55.83±0.18
	Mixup	68.20±0.66	56.33±0.45	60.39±0.40	56.50±0.37	64.24±1.23	57.75±0.80
	NCDG	73.70±0.09	56.48±0.06	70.17±0.04	59.77±0.02	77.78±0.09	63.14±0.06
	EMOE base	73.70±0.07	56.48±0.06	70.17±0.04	59.77±0.02	77.78±0.09	64.89±0.06
	EMOE	<b>75.47±0.09</b>	55.40±0.20	71.28±0.10	<b>60.63±0.17</b>	80.01±0.03	<b>66.14±0.05</b>

selected molecules. We observe the following var@p>0.9 on ChEMBL datasets: EMOE (**0.391**), D-BAT (0.337), EoA (0.301), AdvStyle (0.349), Mixup (0.370), and NCDG (0.239). That is, EMOE is assigning confident predictions to structurally diverse compounds rather than overfitting to a narrow subset of the chemical space.

#### B.4 Full Experiment Results on Tablesift

In Table 8, we report the full results on full results on Tablesift (Gardner, Popovic, and Schmidt 2023) datasets.

Table 7: Full experiment results on ChEMBL (Gaulton et al. 2011) and Therapeutics Data Commons (Huang et al. 2021) datasets. We **bold** best scores based on the mean minus 1 standard deviation. Note that \* refers to a semi-supervised method.

		hERG	A549\_cells	cyp\_2D6	Ames
AUPRC R<0.1	DivDis*	86.92±8.44	89.01±3.53	83.65±6.17	97.47±1.68
	FixMatch*	84.77±1.81	92.93±3.00	92.71±1.98	96.26±1.04
	D-BAT	88.55±1.68	98.57±0.16	95.71±0.89	99.07±0.23
	AdvStyle	93.27±0.56	96.89±0.30	84.21±2.07	99.52±0.12
	EoA	63.80±0.42	61.31±0.31	61.77±0.41	78.74±0.43
	Mixup	82.80±1.56	95.04±0.25	87.39±3.09	91.02±1.05
	NCDG	72.96±1.31	78.79±2.35	61.77±1.15	89.68±0.38
	EMOE base	96.65±0.22	99.74±0.05	<b>99.81±0.11</b>	98.73±0.27
	EMOE	<b>98.10±0.34</b>	<b>99.76±0.03</b>	99.48±0.17	<b>99.66±0.20</b>
AUPRC@ R<0.2	DivDis*	85.65±2.37	89.45±1.16	79.98±1.10	95.80±0.34
	FixMatch*	79.66±0.57	90.81±4.30	83.58±2.55	93.55±0.64
	D-BAT	84.48±1.74	98.26±0.14	91.40±0.98	99.04±0.24
	AdvStyle	88.21±0.77	97.77±0.28	84.83±0.93	<b>99.05±0.17</b>
	EoA	63.80±0.42	61.31±0.31	61.77±0.41	78.74±0.43
	Mixup	82.25±1.51	95.04±0.25	87.09±2.32	91.02±1.05
	NCDG	70.25±1.03	78.22±2.13	61.48±0.98	86.29±0.45
	EMOE base	94.44±0.17	98.22±0.0	95.51±0.19	97.84±0.20
	EMOE	<b>94.67±0.29</b>	<b>98.87±0.09</b>	<b>96.88±0.25</b>	98.45±0.19
AUPRC@ R<0.3	DivDis*	83.69±3.39	88.83±2.50	77.55±1.02	94.87±0.74
	FixMatch*	76.16±1.04	89.12±5.07	77.70±0.205	92.72±0.51
	D-BAT	82.44±1.59	97.37±0.24	87.65±0.58	98.61±0.24
	AdvStyle	85.05±0.86	96.47±0.29	82.76±0.95	<b>98.71±0.20</b>
	EoA	63.80±0.42	61.31±0.31	61.77±0.41	78.74±0.43
	Mixup	81.51±1.35	94.95±0.25	84.53±2.89	90.88±1.00
	NCDG	69.59±0.97	77.88±1.93	60.93±0.86	85.41±0.33
	EMOE base	90.46±0.06	97.35±0.05	92.34±0.24	97.83±0.15
	EMOE	<b>90.88±0.34</b>	<b>97.96±0.1</b>	<b>93.06±0.27</b>	98.18±0.15
AUPRC	DivDis*	67.70±0.25	76.45±0.63	65.76±0.45	82.37±0.27
	FixMatch*	45.16±3.11	51.31±1.28	32.65±2.16	72.54±1.15
	D-BAT	54.60±1.59	67.04±0.53	47.42±0.85	70.44±0.76
	AdvStyle	51.54±0.93	65.02±0.72	44.41±0.96	74.98±0.49
	EoA	43.30±0.51	44.95±0.24	37.37±0.95	59.43±0.18
	Mixup	42.42±0.85	50.52±0.50	27.79±1.49	60.94±0.80
	NCDG	42.69±0.24	49.13±0.79	31.08±0.16	67.79±0.93
	EMOE base	72.19±0.07	84.10±0.01	72.93±0.13	87.43±0.02
	EMOE	<b>73.26±0.08</b>	<b>84.60±0.08</b>	<b>73.59±0.15</b>	<b>88.50±0.10</b>
AUROC	DivDis*	71.19±0.57	72.20±0.41	64.50±0.77	77.05±0.47
	FixMatch*	68.41±0.84	61.16±1.31	80.85±0.40	70.32±0.59
	D-BAT	76.58±0.45	78.16±0.23	67.54±0.47	83.82±0.15
	AdvStyle	75.84±0.46	76.13±0.28	65.51±0.62	<b>85.56±0.71</b>
	EoA	68.02±0.34	68.33±0.24	60.50±0.48	74.77±0.25
	Mixup	73.96±0.26	76.57±0.42	67.53±0.90	78.43±0.49
	NCDG	70.42±0.13	72.50±0.79	62.01±0.16	73.42±0.93
	EMOE base	74.74±0.06	79.17±0.02	70.33±0.07	81.87±0.04
	EMOE	<b>75.97±0.08</b>	<b>79.53±0.06</b>	<b>70.33±0.13</b>	83.78±0.12

Table 8: Full experiment results on Tableshift (Gardner, Popovic, and Schmidt 2023) datasets. We **bold** best scores based on the mean minus 1 standard error. Note that \* refers to a semi-supervised method that uses additional unlabeled OOD data during training.

		Childhood Lead	FICO HELOC	Hospital Readmission	Sepsis
AUPRC@ R<0.1	DivDis*	91.67±3.03	84.88±3.80	88.99±3.36	59.50±1.55
	FixMatch*	86.68±3.32	83.99±2.27	73.97±2.64	17.84±1.87
	D-BAT	52.67±0.00	92.97±0.59	83.73±0.12	81.99±0.33
	AdvStyle	63.63±0.00	90.10±1.03	77.29±0.74	60.79±0.72
	EoA	75.73±0.83	63.42±2.13	52.03±1.78	43.76±1.14
	Mixup	50.00±0.00	92.79±0.03	85.71±0.35	68.21±1.28
	NCDG	83.30±0.20	91.70±0.33	70.42±0.17	72.40±0.04
	EMOE base	98.69±0.03	92.18±0.58	51.31±0.16	82.85±1.53
	EMOE	99.72±0.10	93.93±0.87	66.65±0.17	80.74±1.77
AUPRC@ R<0.2	DivDis*	89.77±2.51	85.50±2.65	83.22±2.57	60.66±1.57
	FixMatch*	81.75±3.69	77.76±1.94	67.84±1.95	17.28±0.58
	D-BAT	62.82±0.00	91.20±0.24	<b>78.84±0.12</b>	75.37±0.38
	AdvStyle	64.96±0.01	88.71±0.65	72.91±0.58	59.83±0.63
	EoA	77.43±0.97	59.53±2.24	51.83±1.66	41.10±1.56
	Mixup	50.00±0.00	91.16±2.10	69.19±3.95	66.09±1.15
	NCDG	82.49±0.18	90.93±0.31	68.88±0.15	70.22±0.03
	EMOE base	97.39±0.06	90.07±0.32	58.30±0.09	<b>78.62±1.57</b>
	EMOE	<b>97.92±0.20</b>	<b>91.72±0.62</b>	67.57±0.12	76.95±1.45
AUPRC@ R<0.3	DivDis*	87.90±2.20	85.77±2.73	79.82±2±42	61.55±1.55
	FixMatch*	81.61±3.09	76.48±4.13	64.47±1.70	18.45±0.46
	D-BAT	68.11±0.00	90.11±0.13	75.26±0.10	70.92±0.44
	AdvStyle	68.67±0.08	87.33±1.21	70.27±0.49	59.02±0.57
	EoA	79.88±1.03	56.52±2.34	51.34±1.27	40.09±1.05
	Mixup	50.00±0.00	90.01±0.02	47.18±3.54	64.41±0.95
	NCDG	82.10±0.15	88.76±0.29	67.52±0.13	69.48±0.03
	EMOE base	96.08±0.08	89.73±0.23	60.86±0.04	75.84±1.55
	EMOE	96.58±0.22	91.10±0.41	67.36±0.06	74.02±1.20
AUPRC	DivDis*	76.33±0.86	82.47±1.05	65.95±2.15	58.85±1.21
	FixMatch*	75.39±0.58	72.22±4.46	56.54±1.21	18.24±0.66
	D-BAT	71.85±0.01	80.91±0.17	63.29±0.08	58.17±0.21
	AdvStyle	48.37±2.77	79.63±1.65	38.13±3.80	54.34±0.27
	EoA	49.48±0.19	59.53±2.24	29.45±4.95	11.21±2.21
	Mixup	50.00±0.00	80.95±0.63	14.15±1.06	56.80±0.40
	NCDG	73.08±0.14	79.05±0.21	58.95±0.10	61.96±0.02
	EMOE base	86.39±0.19	83.80±0.07	62.83±0.03	<b>64.01±0.94</b>
	EMOE	<b>86.70±0.28</b>	<b>84.02±0.09</b>	<b>63.62±0.08</b>	62.21±0.52
AUROC	DivDis*	77.74±1.90	83.55±1.06	65.28±0.59	62.33±0.61
	FixMatch*	79.87±0.29	74.29±1.69	55.78±0.98	49.50±1.01
	D-BAT	79.13±0.02	76.13±0.03	63.22±0.03	57.95±0.04
	AdvStyle	74.45±0.04	77.23±1.69	61.32±0.34	55.31±0.34
	EoA	72.62±0.32	54.67±2.55	51.65±1.70	49.14±2.60
	Mixup	50.00±0.00	78.74±0.17	63.37±0.25	56.82±0.26
	NCDG	76.91±0.13	75.09±0.79	58.67±0.16	<b>63.41±0.93</b>
	EMOE base	84.88±0.19	<b>83.53±0.03</b>	63.18±0.03	62.53±0.82
	EMOE	<b>87.95±0.25</b>	83.11±0.04	<b>63.65±0.07</b>	61.42±0.35

Table 9: Experiment results on PACS dataset. We **bold** best scores based on the mean minus 1 standard deviation.

		PACS dog-elephant	PACS giraffe-horse
AUPRC	D-BAT	58.33 $\pm$ 7.50	82.15 $\pm$ 3.10
④R $\leq$ .1	AdvStyle	54.52 $\pm$ 7.86	88.73 $\pm$ 7.30
	EoA	44.84 $\pm$ 6.95	69.41 $\pm$ 3.66
	Mixup	65.20 $\pm$ 7.80	84.07 $\pm$ 4.53
	EMOE base	<b>66.58<math>\pm</math>1.27</b>	83.23 $\pm$ 0.71
	EMOE	64.00 $\pm$ 1.73	<b>85.90<math>\pm</math>2.92</b>
AUPRC@	D-BAT	58.35 $\pm$ 7.27	80.20 $\pm$ 2.58
④R $\leq$ .2	AdvStyle	55.83 $\pm$ 5.64	84.77 $\pm$ 6.41
	EoA	45.16 $\pm$ 6.39	68.53 $\pm$ 4.25
	Mixup	56.46 $\pm$ 6.74	81.51 $\pm$ 5.45
	EMOE base	60.36 $\pm$ 0.39	82.86 $\pm$ 0.36
	EMOE	<b>61.94<math>\pm</math>1.82</b>	<b>84.10<math>\pm</math>1.44</b>
AUPRC@	D-BAT	57.88 $\pm$ 5.46	78.21 $\pm$ 2.54
④R $\leq$ .3	AdvStyle	56.25 $\pm$ 4.83	81.76 $\pm$ 6.03
	EoA	45.27 $\pm$ 6.21	67.57 $\pm$ 3.79
	Mixup	56.33 $\pm$ 6.51	79.40 $\pm$ 4.96
	EMOE base	58.62 $\pm$ 0.07	<b>82.69<math>\pm</math>0.43</b>
	EMOE	<b>60.80<math>\pm</math>1.44</b>	83.00 $\pm$ 1.35
AUPRC	D-BAT	54.27 $\pm$ 2.78	66.10 $\pm$ 1.74
	AdvStyle	53.52 $\pm$ 2.00	67.94 $\pm$ 3.99
	EoA	45.42 $\pm$ 5.95	68.40 $\pm$ 4.41
	Mixup	54.05 $\pm$ 1.80	67.99 $\pm$ 2.66
	EMOE base	54.47 $\pm$ 0.01	<b>73.10<math>\pm</math>0.64</b>
	EMOE	<b>56.64<math>\pm</math>1.47</b>	72.76 $\pm$ 1.25
AUROC	D-BAT	56.44 $\pm$ 2.66	63.96 $\pm$ 2.38
	AdvStyle	56.24 $\pm$ 1.28	65.88 $\pm$ 3.53
	EoA	49.82 $\pm$ 0.92	54.93 $\pm$ 3.95
	Mixup	57.39 $\pm$ 1.16	64.12 $\pm$ 2.78
	EMOE base	56.94 $\pm$ 0.15	<b>72.86<math>\pm</math>0.61</b>
	EMOE	<b>59.99<math>\pm</math>2.12</b>	72.38 $\pm$ 1.18

## B.5 Full Experiment Results on PACS Dataset

The PACS dataset includes images from four distinct domains: photo, art painting, cartoon, and sketch. Specifically, we focus on the animal classes (dog, elephant, giraffe, and horse) to create 2 challenging binary classification tasks. Models were trained on the ‘photo’, ‘art’, and ‘cartoon’ domains; they were tested on the unseen fourth domain, ‘sketch’, to assess generalization performance. Results on the PACS are shown in In Table 9, we report the full results on images from PACS (Li et al. 2017).

## B.6 Base Experts Ablations

In this section, We ablate the kind of base experts as EMOE NN relies on the base experts to provide pseudo-labels during training. reports the mean AUPRC@R $\leq$ 0.2 across ChEMBL datasets when using XGBoost, Random Forest (with 100 estimators), and Decision Tree as base experts. Performance was comparable between XGBoost and Random Forest, indicating robustness to the choice of strong ensemble models. In contrast, using a weaker base model such as a single Decision Tree led to a performance drop. Nevertheless, EMOE consistently outperformed its respective base experts, demonstrating its ability to enhance predictions re-

Table 10: Mean AUPRC on ChEMBL using D-BAT as EMOE Base.

			hERG	A549_cells	cyp_2D6
AUPRC	D-BAT	86.29	98.37	96.66	
④R $<$ 0.1	EMOE	<b>87.05</b>	<b>98.92</b>	<b>98.51</b>	
AUPRC	EMOE base D-BAT	84.86	97.45	92.56	
④R $<$ 0.2	EMOE	<b>85.66</b>	<b>99.05</b>	<b>95.33</b>	
AUPRC	EMOE base D-BAT	84.12	96.97	89.06	
④R $<$ 0.3	EMOE	<b>84.13</b>	<b>98.01</b>	<b>91.40</b>	
AUPRC	EMOE base D-BAT	72.21	83.79	<b>73.26</b>	
	EMOE	<b>72.73</b>	<b>84.80</b>	73.01	

gardless of base model strength. In addition to the simple models, we conducted ablation on base experts with the most competitive baseline model D-BAT(Pagliardini et al. 2023). We trained 64 D-BAT models each with 5 models in them and apply the same EMOE loss and NN architecture training using this set of base models. Results shows EMOE is able to improve upon complex OOD generalization model like D-BAT (see Tab.10).

## B.7 Per-head Matching Ablation Details

In this section we provide details on the per-head matching ablations where we ablate the matching loss scheme on base experts and explore a mean-only matching approach on expanded points as an alternative. First, we consider utilizing a single-headed (SH) MLP,  $f(x)$  ( $512 \rightarrow 512 \rightarrow 1$ ), which is trained via a mean matching loss  $\mathcal{L}_{\text{MM}}(f, \{g_j\}_{j=1}^K; \mathcal{S}) \equiv \frac{1}{|\mathcal{S}|} \sum_{x \in \mathcal{S}} \ell(f(x), \frac{1}{K} \sum_{j=1}^K g_j(x))$ , rather than the per-expert matching loss,  $\mathcal{L}_{\text{match}}$  (4) We also explored the effect of training our multi-headed (MH) architecture ( $512 \rightarrow 512 \rightarrow 1024$ ) using only mean-matching (without per-head matching),  $\mathcal{L}'_{\text{MM}}(\{h_j\}_{j=1}^K, \{g_j\}_{j=1}^K; \mathcal{S}) \equiv \frac{1}{|\mathcal{S}|} \sum_{x \in \mathcal{S}} \ell(\frac{1}{K} \sum_{j=1}^K \sigma(h_j(x)), \frac{1}{K} \sum_{j=1}^K g_j(x))$ .

## B.8 Bottleneck Ablations Details

Table 11: ChEMBL datasets’ mean AUPRC ablating hidden layer and output sizes.

	④R $<$ .2	④R $<$ 1
Full	97.12	77.28
Full (ML)	96.94	77.25
Full (ERM)	92.65	72.61
Tiny	96.29	76.63
Tiny (ML)	96.33	76.17
Tiny (ERM)	88.28	70.87

In this section, we provide the details and results for the bottleneck ablations. Results are shown in Tab. 11, here ‘Full’ denotes our original  $2 \times 512$  hidden layer architecture, where ‘tiny’ denotes a  $2 \times 32$  hidden layer architecture ( $\times 16$  decrease in parameters). Moreover, we also consider mean logits ‘ML,’ a final averaging over the multi-head logits that produces a single output unit (i.e., averaging the

output weights/bias after training to construct the mean log-its network). The performance gap is marginal between the ‘Full’ and ‘Tiny’ model (a 0.85% difference) when using our proposed loss. In contrast, when using empirical risk minimization, we see a 4.87 times bigger drop in performance between ‘Full’ and ‘Tiny’ models. This suggests that the bottlenecking properties of our method are key to EMOE’s performance. Moreover, the results show promise for EMOE in resource-constrained settings (such as in IoT applications).

## C Additional Figures

Predicted probabilities from EMOE network and base experts. We highlight example instances where the base experts initially makes incorrect predictions but are corrected when we average the predicted probabilities from EMOE network and EMOE base.

## D Limitations

While EMOE consistently improves over its base experts across diverse model types (e.g., XGBoost, Random Forest, Decision Tree, D-BAT), its effectiveness can be influenced by the quality of the base models and the learned latent space. However, our results show that EMOE remains robust even with simpler base models and standard latent representations, suggesting room for further gains with more sophisticated choices. To maintain broad applicability, our experiments were constrained to real-valued vector data with general augmentations. In domain-specific applications, incorporating modality-aware augmentations could further enhance performance. Future work may explore this direction to extend EMOE’s effectiveness.